Micellar Catalysis

DOI: 10.1002/ange.201404729

# Asymmetric Gold-Catalyzed Lactonizations in Water at Room Temperature**

*Sachin Handa, Daniel J. Lippincott, Donald H. Aue, and Bruce H. Lipshutz**

***Abstract:*** *Asymmetric gold-catalyzed hydrocarboxylations are reported that show broad substrate scope. The hydrophobic effect associated with in situ-formed aqueous nanomicelles gives good to excellent ee's of product lactones. In-flask product isolation, along with the recycling of the catalyst and the reaction medium, are combined to arrive at an especially environmentally friendly process.*

Micellar catalysis in water can play an important contributing role in green chemistry. Today, many valued reactions take place within the lipophilic core of self-aggregated nanomicelles, composed of "designer" surfactants tailor-made to best accommodate the synthetic chemistry of interest.[1] The hydrophobic interior of these nanoreactors can function as far more than an alternative, albeit green, solvent for a desired reaction; rather, it offers an opportunity to enhance the binding between a charged catalyst and its counterion, especially in such a characteristically nonpolar environment. Synergistic binding between ions might be leveraged, e.g., in asymmetric gold-catalyzed reactions, which is particularly challenging due to the bicoordinate geometry of $Au^I$. This orientation places a nonracemic ligand distal to its catalytic site,[2] thereby preventing the substrate from attaining the highly biased mode of chelation desired for maximizing enantioselectivity. Nonetheless, a variety of factors have been found leading to asymmetric induction.[2,3] These include the specifics of the ligand–metal binding, such as with Au–arene interactions as well as the nature of the counterion,[4] reaction temperature,[5] and the solvent.[5,6] Ligands such as phosphines,[7] acyclic diaminocarbenes (ADCs),[8] and N-heterocyclic carbenes (NHCs)[9] function well for such Au-catalyzed processes in organic media.

Hydrocarboxylations of olefins and allenes have been found to be highly valuable in the synthesis of target bioactive molecules.[10] Transition metal catalysts, in particular coinage metal-catalyzed enantioselective hydrocarboxylations of allenes forming valuable nonracemic lactones, however, is still an unsolved problem. Indeed, only one simple example is currently known, done in the no longer acceptable solvent benzene and with moderate *ee*.[11] By contrast, related reactions such as intramolecular hydroalkoxylations[5] and hydroaminations[12] of allenes are well established. These are typically done in nonpolar media, and show promising levels of asymmetric induction. Nonetheless, because these reactions, carried out in organic solvents, oftentimes require low temperatures[8,13] to maximize *ee*'s, reaction times can be significantly increased. Moreover, none offers an opportunity to recycle the metal, ligand, or counterion, thus making the overall process both costly and environmentally unattractive.

On the other hand, synergistic binding between catalyst and counterion might be expected due to the hydrophobic effect found within nanomicelles. This could enhance a defined chiral pocket leading to improved enantiocontrol that otherwise is not always observed in traditional organic solvents.[14] Despite these potential advantages to micellar catalysis, no report on asymmetric gold catalysis within such nanoreactors has been reported to date. Herein we describe asymmetric gold-catalyzed intramolecular cyclizations of β-allenic acids[15] to give enantioenriched lactones, carried out within self-aggregated, tailor-made nanoparticles in water at room temperature (Scheme 1).

We started our investigations with allenic acid **1** as a model substrate, looking to find a nonracemic catalyst suitable for use in an aqueous micellar medium. An initial reaction in the designer surfactant TPGS-750M/$H_2O$ with 5 mol% of catalyst *R*-BINAP-$Au_2Cl_2$/AgX afforded **2** in low *ee* (Table 1, entry 1). Altering the axially chiral core of the ligand to $H_8$-BINAP (**4**) and SYNPHOS (**5a**), likewise led to no significant improvement of the *ee* (entries 2 and 3). Increasing the steric bulk of the aromatic residue on

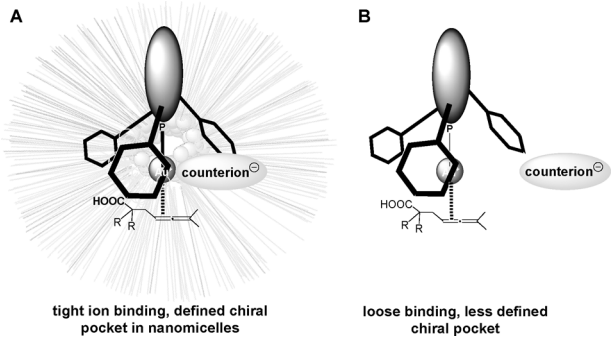


***Scheme 1.*** Cationic gold binding A) within a nanomicellar core in water versus B) in many organic solvents.

[*] Dr. S. Handa, D. J. Lippincott, D. H. Aue, Prof. B. H. Lipshutz
Department of Chemistry & Biochemistry, University of California
Santa Barbara, CA 93106 (USA)
E-mail: lipshutz@chem.ucsb.edu

[**] We acknowledge financial support for our programs in green chemistry, provided by the NIH (GM86485), the Center for Scientific Computing at the CNSI and MRL [NSF MRSEC (DMR-1121053) and NSF CNS-0960316], and NSF support from the National Center for Supercomputing Applications (NSF TG-CHE100123) utilizing the NCSA Gordon and Blacklight systems. We thank Prof. L. Slaughter (U North Texas) for sharing experimental procedures leading to some of the allenic acids utilized in this work, and Eric D. Slack for technical assistance.

Supporting information for this article is available on the WWW under http://dx.doi.org/10.1002/anie.201404729.

  

***Table 1:*** Optimization of Au-catalyzed asymmetric intramolecular hydrocarboxylations of allenic acids.

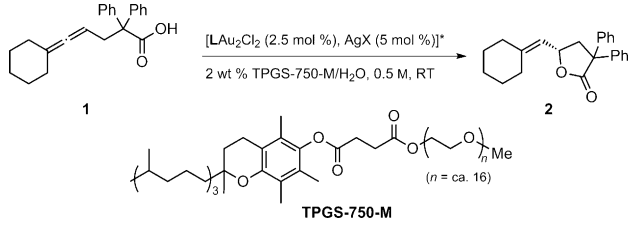


| Entry | Ligand **L** | $X^-$ | *t* [h] | Yield **2** | *ee* [%] |
|---|---|---|---|---|---|
| 1 | **3** | $BF_4$ | 78 | 98 | 3 |
| 2 | **4** | $SbF_6$ | 74 | 95 | 11 |
| 3 | **5a** | $SbF_6$ | 72 | 95 | 18 |
| 4 | **5b** | $SbF_6$ | 78 | 96 | 30 |
| 5 | **7** | $SbF_6$ | 29 | 93 | 1 |
| 6 | **8** | $SbF_6$ | 32 | 92 | 7 |
| 7 | **9** | PMB | 67 | 67 | 40 |
| 8 | **9** | PNB | 70 | 70 | 50 |
| 9 | **10** | $SbF_6$ | 60 | 85 | 29 |
| 10 | **11a** | $SbF_6$ | 70 | 90 | 6 |
| 11 | **11b** | $SbF_6$ | 75 | 91 | 36 |
| 12 | **11c** | $SbF_6$ | 42 | 94 | 7 |
| 13 | **11d** | PNB | 72 | 95 | 51 |
| 14 | **12a** | $SbF_6$ | 48 | 95 | 12 |
| 15 | **12b** | $SbF_6$ | 49 | 91 | 18 |
| 16 | **12c** | $SbF_6$ | 40 | 85 | 31 |
| 17 | **12d** | PNB | 30 | 97 | 37 |
| 18 | **12e** | PNB | 38 | 70 | 30 |
| **19** | **12f** | **PNB** | **48** | **97** | **55** |

*$LAu_2Cl_2$ = LAuCl (5 mol %) when **L** = **7**, **8**, and **9**. PNB = *p*-nitrobenzoate, PMB = *p*-methoxybenzoate. For ligands, see Scheme 2. For a detailed optimization Table, see SI.

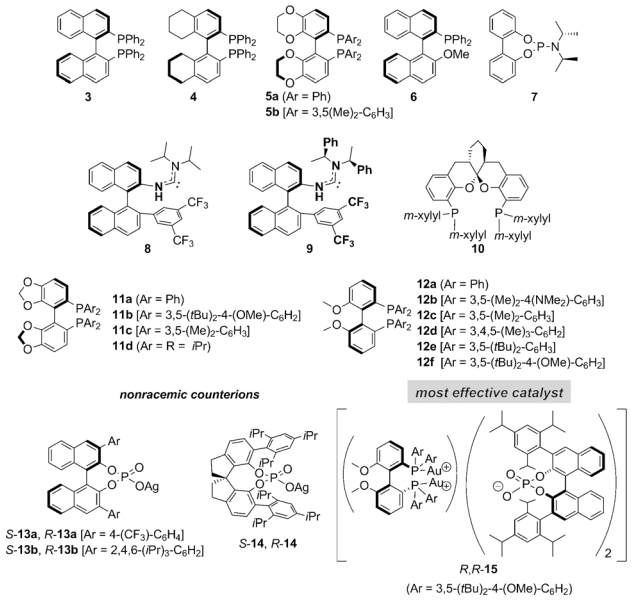


***Figure 1.*** Ligands and counterions used for optimization studies.

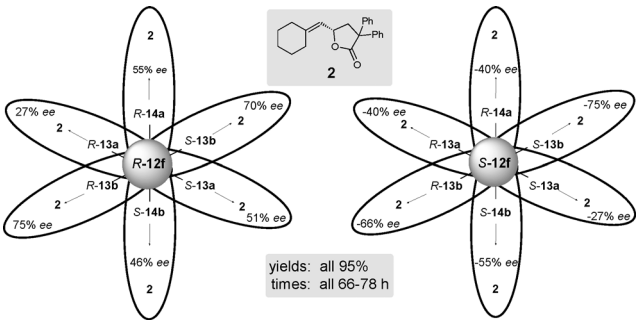


***Scheme 2.*** Venn diagram showing match/mismatch combinations between ligand **12f** and counterions.

phosphorus contributes toward the observed enantioselectivity, as 3,5-Xyl-SYNPHOS (**5b**) increased the *ee* to 30% (entry 4). The improvement in *ee* due to steric effects near the donor atom of the ligand suggested the use of monodentate ligands, including phosphoramidite **7** and ADCs **8** and **9**. Interestingly, an increased *ee* to 50% was only seen with the larger ADC **9**. The choice of counterion also affected the selectivity of the reaction (entries 7 and 8). No significant improvements in terms of *ee* were observed even with further alterations in the axially chiral core of several bis-phosphine ligands (entries 9–12). A 51% *ee* was obtained using SEGPHOS ligand **11d** when accompanied by *p*-nitrobenzoate as a counterion (entry 13). The best results were obtained by the fine-tuning of BIPHEP ligands (entries 14–19), with **12f** being identified as the best choice so far (entry 19). In the absence of surfactant there was essentially no reaction.

The impact of counterions on both *ee*'s and yields in aqueous micelles suggested that further tuning of a catalyst system with focus on the chiral counterion might be productive. Initial match/mismatch studies were performed on both *R* and *S* enantiomers of methoxy-BIPHEP ligand **12f**, with counterions *S*-**13a**, *R*-**13a**, *S*-**13b**, *R*-**13b**, *S*-**14a**, and *R*-**14a** (Figure 1). A significant mismatch was found between ligand *R*-**12f** and counterion *R*-**13a** giving only 27% *ee* of product **2**, whereas the enantiomeric counterion *S*-**13a** led to an *ee* of 51% (Scheme 2). Using a far bulkier BINOL-based counterion *S*-**13b**, an insignificant match/mismatch existed, as only a 5% difference in *ee* was obtained in product **2** (75% vs. 70%). An *ee* of 66% was found in the reaction of **1** using *S*-**12f**-$Au_2$ and counterion *R*-**13b**-Ag. Spirocyclic phosphate counterion **14** provided slightly better results in terms of *ee* than did counterion **13a**. In order to find the best match for an active catalyst, additional reactions were performed using *S*-**12f**-$Au_2$, along with both enantiomers of silver salts of **13a**,**b** and **14**. Interestingly, no general trend of match/mismatch between catalyst **12f** and different counterions was observed. From all combinations studied using the model reaction, the combinations *R*-**12f**-$Au_2$/*R*-**13b**-Ag or *S*-**12f**-$Au_2$/*S*-**13b**-Ag (75% *ee*) was found to be the best pair between ligand **12f** and counterions **13a**, **13b**, and *S*- or *R*-**14**.

Using the catalyst system containing ligand *R*-**12f** and a counterion *R*-**13b**, further optimization studies were undertaken. These revealed a dependence of the *ee* on several variables, including 1) Au-nanoparticle-free conditions; 2) the nature of acidic or basic additives; 3) the presence of AgCl; 4) the ratio of $(L\text{-AuCl})_2$ to AgX; 5) removal of both chloride ions attached to gold; 6) protection from ambient light; 7) the purity of the catalyst and counterion; 8) the

  

surfactant concentration, and 9) the reaction temperature (see the Supporting Information (SI) for details). Optimal reaction conditions were found to be: 3 wt% TPGS-750M as surfactant in water as the reaction medium, breaking of the crystallinity of solids by the addition of minimal amounts of solvent additives, use of 3 mol% of AgCl-free, pure active gold-catalyst *R*,*R*-**15**, 0.5 M global concentration, extraction of the product with a minimum amount of 10% ether in hexanes to maximize the amount of catalyst that remains in the aqueous medium in the reaction vessel, and ambient temperature.

Under these optimized conditions, including the "trick" of softening highly crystalline solid substrates with a drop or two of an organic solvent (DMSO, benzene, or toluene) as "additive", reaction times were decreased significantly; in the case of starting material **1**, from 72 to 16 h. The *ee* could be increased from 75% to 88% by using isolated AgCl-free catalyst *R*,*R*-**15**. The X-ray structure of *R*,*R*-**15** shows the defined chiral pocket with weak Au–arene interactions (Figure 2). The binding between the cationic gold and the counterion through the phosphate group supports the match between them, which had already been determined experimentally (see above).

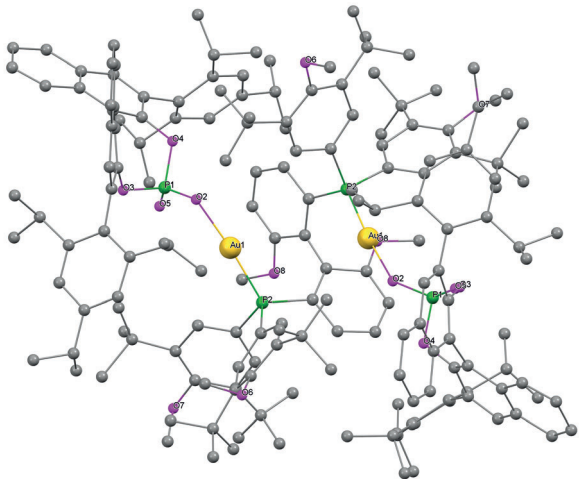

***Figure 2.*** X-ray structure of *R*,*R*-**15** in ball and stick. Color code: C, gray; O, purple; P, green; Au, yellow.

As illustrated in Scheme 3, a variety of precursor allenic acids were cyclized to afford high yields of product lactones. This new technology is clearly applicable to many substitution patterns associated with both the allenic group as well as the α-carbon of the carboxylic acid. Unsubstituted as well as dialkyl-substituted allenic termini appear to give *ee*'s that are among the highest observed (81–92%). Allenes bearing saturated rings at the terminus ranging from five- to eight-membered in size afforded ee's that were more variable, and seemingly dependent on the nature of the substituent(s) at the α-carbon. Most *ee*'s are in the 80–90% range, and hence, it is unclear why spirocyclic lactone **23** was formed in 96% *ee*. With a single substituent α to the acid, diastereomers are formed; the major isomer **32** was isolated (48%) and has an *ee*

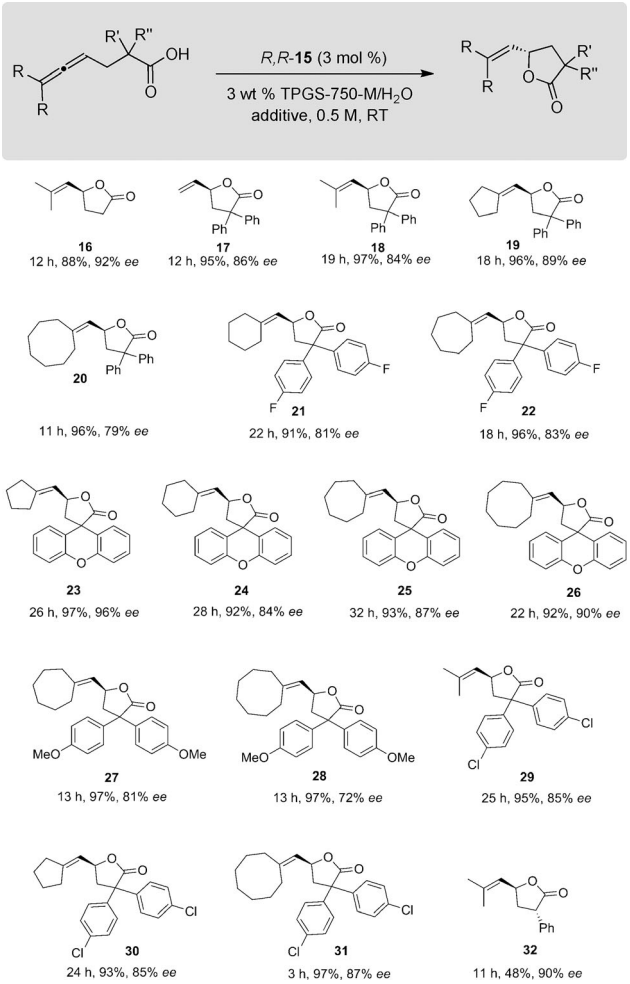


***Scheme 3.*** Substrate scope (additive = trace amounts of organic solvent).

of 90%. The other diastereomer underwent secondary processes leading to unidentifiable material.

To confirm that the solvent additive is acting solely to soften the highly crystalline nature of the substrates and the catalyst, and neither impacting the role of the micellar environment nor merely acting as the reaction medium, the highly crystalline substrate **33** was subjected to the reaction conditions in different reaction media including neat DMF, DMSO, and toluene as well as in TPGS-750-M with these same solvent additives (Scheme 4). Similar *ee*'s were observed when reactions were run in aqueous TPGS-750-M with solvent additives, whereas different *ee*'s were obtained in each of the neat organic solvents. Poorer *ee*'s in polar organic solvents and better *ee*'s in nonpolar organic solvents and

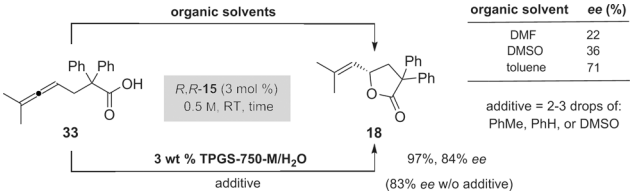


***Scheme 4.*** Impact of the reaction medium on the *ee*.

TPGS-750-M are indicative of the surfactant serving as the reaction medium, providing the hydrophobic effect inside the micellar core (for details, see SI).

The progress of a representative reaction of allenic acid **33** leading to lactone **18** under the influence of the cationic gold catalyst *R*,*R*-**15** was followed over time. As the reaction progressed, the *ee* of **18** remained constant, as determined by HPLC analyses of several aliquots. The absolute stereochemistry of the newly created center in the product was determined by single-crystal X-ray diffraction analysis, clearly indicating *S*-stereochemistry (Figure 3).

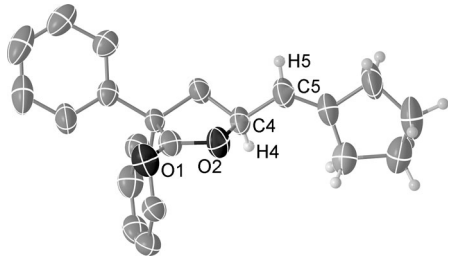


***Figure 3.*** X-ray structure of *S*-**19**.

The mechanism by which these Au-catalyzed reactions might proceed has been investigated with DFT calculations, using a $PH_3$ ligand and the carboxylic acid precursor of **19** without phenyl substituents. The calculations showed that direct 5-*exo*-trig cyclization of **A** to form a protonated lactone **E** was substantially uphill, $\Delta G° = 13.2$ kcal mol$^{-1}$ in toluene (Scheme 5). The 6-*endo*-dig complex was uphill by 10.7 kcal

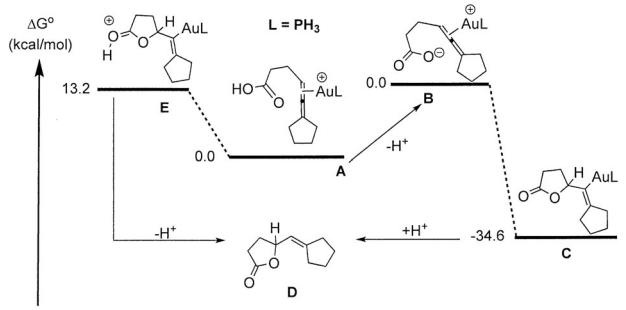


***Scheme 5.*** Plausible mechanism with DFT energy diagram at the PBE1PBE/6-31 + G(d,p)/SDD(Au)/SMD(toluene) level of theory with relative free energies in toluene at 298 K in kcal mol$^{-1}$. The free energy difference between **A** and **B** depends on the base used and is not well known in the micellar media (see SI).

mol$^{-1}$e, whereas the 6-*exo*-dig and 7-*endo*-trig products were uphill by 22.6 and 18.8 kcal mol$^{-1}$, respectively [PBE1PBE/6-31 + G(d,p)/SDD(Au)/SMD(toluene)]. On the other hand, cyclization reactions of the deprotonated complex **B** were downhill energetically by 22.1 kcal mol$^{-1}$ for the 5-*exo*-trig cyclization and 21.9 kcal mol$^{-1}$ for the 6-*endo*-dig cyclization in dichloromethane (see SI). In toluene, these free energies were considerably larger, 34.6 and 35.2 kcal mol$^{-1}$, respectively, as expected. These observations, together with the fact that the addition of catalytic triethylamine or quaternary ammonium hydroxides substantially accelerated the reactions in the micelle, suggests that the reaction with base may proceed via the deprotonated complex **B** to form **C**. After deprotonation of the carboxylic acid group in the gold–allene complex, the cyclization occurs with little or no barrier in our theoretical modeling. Reaction trajectory modeling is consistent with the observed preference for 5-*exo*-trig cyclization. This mechanism is in stark contrast to the mechanism proposed for the gold-catalyzed cyclization of allenic alcohols, with reversible cyclization and rate-determining protodeauration,[16] but the reactions in the absence of added base may occur via **E** rather than **B**. The calculated transition-state energies for cyclization by this pathway also show a preference for the 5-*exo*-trig pathway. Such a change of mechanism would be consistent with our observation that a low *ee* is observed in reactions with a chiral counterion in the presence of added triethylamine.

Studies were also conducted to assess the potential for recycling of the aqueous medium. Given that our portfolio of "designer" surfactants are engineered to remain in the water,[16] the more intriguing question concerned the fate of the gold catalyst with respect to both its recyclability as well as its efficacy. Upon extraction with minimal amounts of 10% ether in hexanes, more than 50% of the catalyst remained in the aqueous phase such that only 1 mol% of fresh *R*,*R*-**15** need be added at each cycle. As illustrated in Scheme 6, the *ee*'s for product **2** remained essentially constant, as did the yields, throughout six successive recycles. The associated E Factor based on organic solvent usage,[17,18] as a measure of the "greeniness" of this protocol was calculated to be only 4.9, which compares very well with values typically seen from chemistry done in the fine chemicals and pharma arenas.[17]

In summary, the hydrophobic effect characteristic of nanomicelles has been utilized advantageously to enhance tight ion-pair binding between a nonracemic cationic gold catalyst and its nonracemic counterion. This combination is highly effective in achieving especially challenging asymmetric intramolecular hydrocarboxylation of allenes in high yields and good to excellent *ee*'s. The aqueous micellar reaction medium obviates the use of organic solvents, and

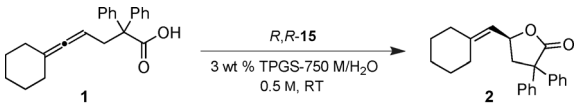


**Recycling of the reaction medium**

| Run | *R*,*R*-**15** [mol %] | Yield **2** [%] | *ee* **2** [%] |
|---|---|---|---|
| 0 | 3 | 97 | 86 |
| 1 | 1 | 97 | 86 |
| 2 | 1 | 96 | 86 |
| 3 | 1 | 97 | 85 |
| 4 | 1 | 95 | 85 |
| 5 | 1 | 96 | 85 |
| 6 | 1 | 96 | 85 |

$$\text{E Factor} = \frac{\text{organic waste (kg)}}{\text{product (kg)}} = 4.9$$

***Scheme 6.*** Studies on recycling and E Factor.

  

both the catalyst and surfactant can be recycled. The associated E Factor for the overall process is very low, documenting its environmentally friendly nature.

Received: April 26, 2014
Revised: July 12, 2014
Published online: August 14, 2014

**Keywords:** asymmetric catalysis · gold catalysis · micellar catalysis · surfactants

[1] B. H. Lipshutz, S. Ghorai, *Aldrichimica Acta* **2012**, *45*, 3.
[2] A. S. K. Hashmi, *Angew. Chem.* **2005**, *117*, 7150; *Angew. Chem. Int. Ed.* **2005**, *44*, 6990.
[3] a) Z. Li, C. Brouwer, C. He, *Chem. Rev.* **2008**, *108*, 3239; b) K. Yavari, P. Aillard, Y. Zhang, F. Nuter, P. Retailleau, A. Voituriez, A. Marinetti, *Angew. Chem.* **2014**, *126*, 880; *Angew. Chem. Int. Ed.* **2014**, *53*, 861; c) R. A. Widenhoefer, *Chem. Eur. J.* **2008**, *14*, 5382; d) N. Huguet, A. M. Echavarren, *Asymmetric Synthesis II: More Methods and Applications*, Wiley-VCH, Weinheim, **2013**, pp. 205 – 211; e) A. Fürstner, *Acc. Chem. Res.* **2014**, *45*, 925; f) P. Gu, Q. Xu, M. Shi, *Tetrahedron Lett.* **2014**, *55*, 577.
[4] a) Y.-M. Wang, A. D. Lackner, F. D. Toste, *Acc. Chem. Res.* **2014**, *47*, 889; b) I. Caracelli, J. Zukerman-Schpector, E. R. Tiekink, *Gold Bull.* **2013**, *46*, 81; c) S. Handa, L. M. Slaughter, *Angew. Chem.* **2012**, *124*, 2966; *Angew. Chem. Int. Ed.* **2012**, *51*, 2912; d) K. Ohmatsu, M. Ito, T. Kunieda, T. Ooi, *Nat. Chem.* **2012**, *4*, 473; e) R. J. Phipps, G. L. Hamilton, F. D. Toste, *Nat. Chem.* **2012**, *4*, 603; f) K. Aikawa, M. Kojima, K. Mikamia, *Adv. Synth. Catal.* **2010**, *352*, 3131; g) J Lacour, D. Moraleda, *Chem. Commun.* **2009**, 7073; h) K. Aikawa, M. Kojima, K. Mikami, *Angew. Chem.* **2009**, *121*, 6189; *Angew. Chem. Int. Ed.* **2009**, *48*, 6073; i) S. Mukherjee, B. List, *J. Am. Chem. Soc.* **2007**, *129*, 11336; j) T. Ooi, K. Maruoka, *Angew. Chem.* **2007**, *119*, 4300; *Angew. Chem. Int. Ed.* ***2007***, *46*, 4222; k) J. Lacour, V. Hebbe-Viton, *Chem. Soc. Rev.* **2003**, *32*, 373.
[5] Z. Zhang, Z. R. A. Widenhoefer, *Angew. Chem.* **2007**, *119*, 287; *Angew. Chem. Int. Ed.* **2007**, *46*, 283.
[6] C. Liu, R. A. Widenhoefer, *Org. Lett.* **2007**, *9*, 1935.
[7] a) Y. Ito, M. Sawamura, T. Hayashi, *J. Am. Chem. Soc.* **1986**, *108*, 6405; b) Y. W. Sun, Q Xu, M. Shi, *Beilstein J. Org. Chem.* **2013**, *9*, 2224; c) S. Sengupta, X. Shi, *ChemCatChem* **2010**, *2*, 609; d) Z. M Zhang, P. Chen, W. Li, Y. Niu, X. Zhao, J. Zhang, *Angew. Chem.* **2014**, *126*, 4439; *Angew. Chem. Int. Ed.* **2014**, *53*, 4350.
[8] a) H. G. Raubenheimer, *Angew. Chem.* **2012**, *124*, 5128; *Angew. Chem. Int. Ed.* **2012**, *51*, 5042; b) L. M. Slaughter, *ACS Catal.* **2012**, *2*, 1802; c) M. Barbazanges, L. Fensterbank, *ChemCatChem* **2012**, *4*, 1065; d) G. Cera, M. Bandini, *Isr. J. Chem.* **2013**, *53*, 848.
[9] a) J. Francos, F. Grande-Carmona, H. Faustino, J. Iglesias-Sigüenza, E. Díez, I. Alonso, R. Fernández, J. M. Lassaletta, F. López, J. L. Mascareñas, *J. Am. Chem. Soc.* **2012**, *134*, 14322; b) P. Gu, X. Xu, M. Shi, *Tetrahedron Lett.* **2014**, *55*, 577.
[10] V. Andrushko, N. Andrushko, *Stereoselective Synthesis of Drugs and Natural Products II*, Wiley-VCH, Weinheim, **2013**, pp. 1280 – 1836.
[11] a) J. L. Arbour, H.S Rzepa, J. Contreras-García, L. A. Adrio, E. M. Barreiro, K. K. Hii, *Chem. Eur. J.* **2012**, *18*, 11317; b) G. L. Hamilton, E. J. Kang, M. Mba, F. D. Toste, *Science* **2007**, *317*, 496.
[12] Z. Zhang, C. F. Bender, R. A. Widenhoefer, *J. Am. Chem. Soc.* **2007**, *129*, 14148.
[13] Z. Zhang, C. F. Bender, R. A Widenhoefer, *Org. Lett.* **2007**, *9*, 2887.
[14] S. Huang, K. R. Voigtritter, J. B. Unger, B. H. Lipshutz, *Synlett* **2010**, 2041.
[15] This class of allenic acid substrates has recently been developed in related lactonization reactions catalyzed by achiral gold complexes; see S. Handa, Ph-D. thesis, Oklahoma State University (USA), **2013**.
[16] T. J. Brown, D. Weber, M. R. Gagné, R. A. Widenhoefer, *J. Am. Chem. Soc.* **2012**, *134*, 9134.
[17] B. H. Lipshutz, N. A. Isley, J. C. Fennewald, E. D. Slack, *Angew. Chem.* **2013**, *125*, 11156; *Angew. Chem. Int. Ed.* **2013**, *52*, 10952.
[18] a) R. A. Sheldon, I. W. C. E. Arends, U. Hanefeld, *Green Chemistry and Catalysis*, Wiley-VCH, Weinheim, **2007**, pp. 1 – 47; b) R. A. Sheldon, *Green Chem.* **2007**, *9*, 1273.